



Gapped Surface States in a Strong-Topological-Insulator Material

A. P. Weber,^{1,*} Q. D. Gibson,² Huiwen Ji,² A. N. Caruso,¹ A. V. Fedorov,³ R. J. Cava,² and T. Valla⁴

¹*Department of Physics and Astronomy, University of Missouri-Kansas City, Kansas City, Missouri 64110, USA*

²*Department of Chemistry, Princeton University, Princeton, New Jersey 08544, USA*

³*Advanced Light Source, Lawrence Berkeley National Laboratory, Berkeley, California 94720, USA*

⁴*Condensed Matter Physics and Materials Science Department, Brookhaven National Laboratory, Upton, New York 11973, USA*

(Received 21 January 2015; published 23 June 2015)

A three-dimensional strong-topological insulator or semimetal hosts topological surface states which are often said to be gapless so long as time-reversal symmetry is preserved. This narrative can be mistaken when surface state degeneracies occur away from time-reversal-invariant momenta. The mirror invariance of the system then becomes essential in protecting the existence of a surface Fermi surface. Here we show that such a case exists in the strong-topological-semimetal Bi_4Se_3 . Angle-resolved photoemission spectroscopy and *ab initio* calculations reveal partial gapping of surface bands on the Bi_2Se_3 termination of $\text{Bi}_4\text{Se}_3(111)$, where an 85 meV gap along $\bar{\Gamma}\bar{K}$ closes to zero toward the mirror-invariant $\bar{\Gamma}\bar{M}$ azimuth. The gap opening is attributed to an interband spin-orbit interaction that mixes states of opposite spin helicity.

DOI: [10.1103/PhysRevLett.114.256401](https://doi.org/10.1103/PhysRevLett.114.256401)

PACS numbers: 71.20.-b, 71.70.Ej, 73.20.At, 79.60.Bm

Topological insulator materials (TIM) [1], which include insulators [2–4] and semimetals [5–10], possess an inverted bulk band gap that hosts unusually robust, spin-helical topological surface states (TSS) at the material’s boundaries. The presence of TSS is guaranteed by the topology of the bulk bands and the states can only be removed from the Fermi energy if protecting symmetries are broken. Strong topological insulator (STI) [11,12] materials hold a special distinction, as they are often said to host gapless TSS protected by time-reversal symmetry (TRS) on every surface termination of the crystal. We will show it is possible for the TSS of material in a STI phase to intrinsically acquire a finite gap at all momenta in the surface Brillouin zone (SBZ) which do not lie on a mirror-invariant azimuth. In that case, the mirror symmetry (MS) of the crystal lattice must be intact to guarantee the existence of a surface Fermi surface. Earlier work by Teo, Fu, and Kane [13] had foreseen this possibility; however, no concrete examples have been obtained in experiment. Here, we show that such a system exists in the strong-topological-semimetal Bi_4Se_3 . The finding of mirror-protected TSS in this system also provides direct confirmation that the strong-topological-insulator phase can coexist with the topological-crystalline-insulator phase of matter, as was suggested by Rauch *et al.* [14] for the case of Bi chalcogenides.

Bi_4Se_3 is a rhombohedral superlattice material consisting of alternating Bi_2 and Bi_2Se_3 layers stacked along the (111) direction. Previously, Dirac conelike TSS were found in the gap between the first fully occupied bulk valence band (BVB) and the holelike bulk conduction band (HCB) on two different surface terminations of $\text{Bi}_4\text{Se}_3(111)$ [10]. It was determined that the TSS result from a parity inversion at the $\bar{\Gamma}$ point of the bulk Brillouin zone (BBZ),

a characteristic shared with the Bi_2Se_3 parent compound [15]. Although effects of hybridization between surface and bulk electrons were mentioned, it was not made clear that the states of the upper Dirac cone appearing on the Bi_2Se_3 -terminated surface, which have an electronlike dispersion, must have crossed the HCB to reach the Fermi level. The possibility of new topological constraints on the surface electron structure above the HCB was also not explored. Earlier work [9] predicted that the band gap above the HCB is characterized by a single parity inversion at the F point of the BBZ, which demands that TSS within this gap must come in an odd number of pairs [13]. If that is the case, then an odd number of surface bands must appear within the gap to meet the state which crossed the HCB. Moreover, this parity inversion is away from the center of the BBZ and the crystal does not cleave at the center of inversion. Under these conditions, the TSS pairs are not constrained to have Dirac points at time-reversal invariant momenta (TRIM) [13].

Consistent with the prediction in Ref. [9], it is in the momentum-space region outside the HCB edge that evidence of partially gapped TSS is found through *ab initio* calculations and angle-resolved photoemission spectroscopy (ARPES) measurements on the Bi_2Se_3 -terminated surface of $\text{Bi}_4\text{Se}_3(111)$. The TSS degenerate away from TRIM on the mirror-invariant $\bar{\Gamma}\bar{M}$ azimuth in the SBZ. The bands become separated elsewhere, and an 85 meV gap between the surface state branches is measured along $\bar{\Gamma}\bar{K}$ in ARPES. The origin of this gap is accounted for in a model for the spin-orbit interaction on a (111) crystal surface. These findings place 2D electron hybridization within the subject of pristine STI materials and provide direct evidence for MS protection of surface states in a Bi chalcogenide.

Single crystals of Bi_4Se_3 were synthesized following a previously reported procedure [10]. ARPES was performed using a Scienta SES-100 electron spectrometer at beam line 12.0.1 of the Advanced Light Source with a combined instrumental energy resolution of ~ 12 meV and an angular resolution better than $\pm 0.07^\circ$. The sample was cleaved under ultrahigh vacuum conditions ($< 5.0 \times 10^{-9}$ Pa) and kept at ~ 15 K. Temperature was measured using a silicon sensor mounted near the sample.

Electron structure calculations were performed in the framework of density-functional theory (DFT) using the WIEN2K code [16] with a full-potential linearized augmented plane-wave and local orbitals basis together with the Perdew-Burke-Ernzerhof [17] parametrization of the generalized gradient approximation, using a slab geometry. Experimentally determined lattice parameters and atom positions were used to construct the slabs. The plane-wave cutoff parameter $R_{\text{MT}}K_{\text{max}}$ was set to 7 and the Brillouin zone was sampled by 9 k points. Spin-orbit coupling (SOC) was included. To study the Bi_2Se_3 -terminated surface, a slab was constructed of 6 Bi_2Se_3 layers and 5 Bi_2 layers, with 10 Å of vacuum between adjacent slabs. The contribution of the surface atoms to the overall surface electronic structure was determined by calculating the partial contribution of each atomic basis set to the wave functions at all k points.

The calculated electron structure for Bi_2Se_3 -terminated slabs of $\text{Bi}_4\text{Se}_3(111)$ is shown in Fig. 1. A surface state crossing protected by MS only is indicated by the red circle and the blue circle indicates a crossing which is “dually protected” [14] by both MS and TRS. The TSS within the blue-circled region lie between the BVB and HBCB. These TSS were the primary focus of previous investigations [9,10]. The TSS that cross within the red-circled region, which are the focus of the present work, lie above the HBCB. The parity invariants of the bulk band structure counted up to the HBCB were previously determined to be +1, +1, +1, and -1 at the Γ , Z , L , and F points of the BBZ, respectively [9]. The product of the parity invariants is -1, which characterizes the gap above the HBCB as a STI type [11,12]. Applying the methods of Ref. [13] to our case, an odd number of TSS pairs are expected to exist between the surface projections of F (\bar{M}) and Γ ($\bar{\Gamma}$). Indeed, we observe a single pair of TSS that cross each other along the $\bar{\Gamma}\bar{M}$ azimuth and degenerate with different ends of the bulk gap at $\bar{\Gamma}$ and \bar{M} . Group-theoretical considerations indicate why this crossing is allowed even while the surface states are seen to be gapped along the $\bar{\Gamma}\bar{K}$ azimuth.

At the (111) surface, the $R\bar{3}m$ symmetry of the crystal reduces to C_{3v} . For wave vectors lying between $\bar{\Gamma}$ and \bar{M} , the point-group symmetry reduces to C_s , which contains two irreducible representations characterized by mirror eigenvalues of $\pm i$. Through the definition of the mirror operation [13], it is easily shown that the two irreducible representations correspond to states of opposite spin helicity, which cannot hybridize with each other on the

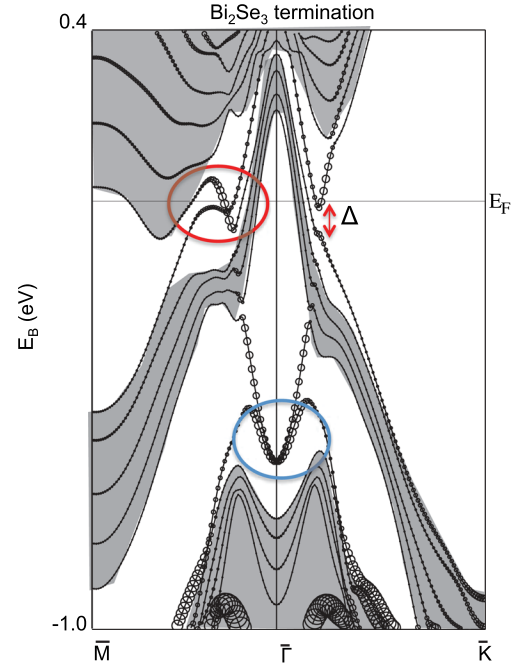


FIG. 1 (color online). Calculated band structure for the Bi_2Se_3 -terminated slabs of Bi_4Se_3 plotted along the $\bar{M}\bar{\Gamma}\bar{K}$ path in the surface Brillouin zone. The size of the circular plotting markers indicates the contribution from the surface layer. Shaded regions indicate the projection of bulk electrons. The red circle contains the mirror-symmetry-protected crossing of TSS and the red double arrow indicates the corresponding TSS avoided crossing gap Δ . The blue circle contains a TSS crossing protected by both TRS and MS.

mirror-invariant $\bar{\Gamma}\bar{M}$ azimuth. This explains why the crossing circled in red is allowed and, indeed, protected by the crystal’s mirror symmetry. In contrast, the point group of the wave vectors along $\bar{\Gamma}\bar{K}$ is C_1 . By symmetry, crossings between $\bar{\Gamma}$ and \bar{K} are avoided, even for states of opposite spin helicity. The same is true for all wave vectors in the SBZ which do not lie on a mirror-invariant azimuth. The double arrow in Fig. 1 indicates what can therefore be understood as a hybridization gap Δ resulting from the avoided crossing of spin-helical surface states, as will be discussed later. Note that the combination of C_3 and time-reversal symmetry imply that the surface Fermi surface will consist of six *equivalent* pockets that each enclose a surface state degeneracy point. This observation is consistent with the definition of a STI material as put forward by Teo, Fu, and Kane [13].

The k dependence of the gapped structure results from competing SOC interactions which couple to different components of the spin degree of freedom. This can be captured in a model for the SOC Hamiltonian $H_{\text{SOC}} \propto (\vec{p} \times \vec{\nabla}V) \cdot \vec{\sigma}$ using $k \cdot p$ theory. Polar coordinates are chosen with $\bar{\Gamma}$ as the origin and θ denoting the in-plane azimuthal angle from the k_x axis, aligned to the $\bar{\Gamma}\bar{K}$ direction. If the energy splitting of the TSS near $k = 0$

is taken to equal $2v\kappa$, then H_{SOC} to first order in k couples the in-plane, tangential component of spin $\langle\sigma_t\rangle$ to the out-of-plane electrostatic potential gradient with a strength v as $H_1(\vec{k}) \equiv v(k - \kappa)\sigma_t$. To third order in k , there appears a second term [18] that couples the out-of-plane component of spin to the in-plane crystalline potential gradient with a strength λ as $H_2(\vec{k}) \equiv \lambda k^3 \cos(3\theta)\sigma_z$. Together,

$$H_{\text{SOC}}(\vec{k}) = \begin{bmatrix} \lambda k^3 \cos(3\theta) & iv(k - \kappa)e^{-i\theta} \\ -iv(k - \kappa)e^{i\theta} & -\lambda k^3 \cos(3\theta) \end{bmatrix}$$

and we find the spin-orbit contribution to the dispersion

$$E_{\text{SOC}}(\vec{k})_{\pm} = \pm \sqrt{v^2(k - \kappa)^2 + \lambda^2 k^6 \cos^2(3\theta)},$$

where we refer to $+$ and $-$ as the upper Dirac branch (UDB) and lower Dirac branch (LDB), respectively. At $k = \kappa$, the magnitude of the gap between the DBs is determined solely by the second term under the square root. The gap carries the sign of an f wave, which changes at the mirror-invariant azimuths, signifying a change in the z polarizations of the DBs (this could alternately be described as a crossing of bands with positive and negative z polarization). The sign appears in the interband matrix element,

$$\Delta = \langle - | H_2(\vec{k}) | + \rangle = -2\lambda k^3 \cos(3\theta),$$

for the spin-helical states typically invoked in the discussion of simple, gapless TSS. In this sense, the crystalline anisotropy should cause an interband SOC effect that gives rise to the gapped structure. The model only differs from the TSS of the STI Bi_2Te_3 [18] in the location of the Dirac point. No extra bands need to be inferred to achieve the complex, partially gapped TSS described below.

Figure 2 displays electron structure calculated from the model Hamiltonian, for which we have chosen the values $v = 5.5 \text{ eV}\text{\AA}$, $\lambda = 55 \text{ eV}\text{\AA}^3$, $\kappa = 0.25 \text{ \AA}^{-1}$ in rough approximation of the Bi_2Se_3 termination electron structure. The reader should note the many omissions from this model such as spin-orbital entanglement (which will disallow a pure spin-eigenstate character for the TSS and limit the magnitude of spin polarization) [19], and higher-order interaction terms [20]. Figure 2(a) shows the spin-resolved band structure along the $\theta = 0$ azimuth, with the bands corresponding to the case $\lambda = 0$ plotted in black. The minimum energy gap δ is located inside of $k = \kappa$, and we find it is the case that at $k_{\delta} \leq \kappa$ for all θ , as shown in panel 2(c). It is telling to inspect the in-plane helical spin polarization, indicated by color scale, relative to the magnitude of the out-of-plane polarization, indicated by marker size. For $k < 0.1 \text{ \AA}^{-1}$, the spin is helical, but as the contribution of H_2 grows, the deviation from linear dispersion is accompanied by increasing z polarization. At k_{δ} , the contribution of H_2 overtakes that of H_1 . At $k = \kappa$,

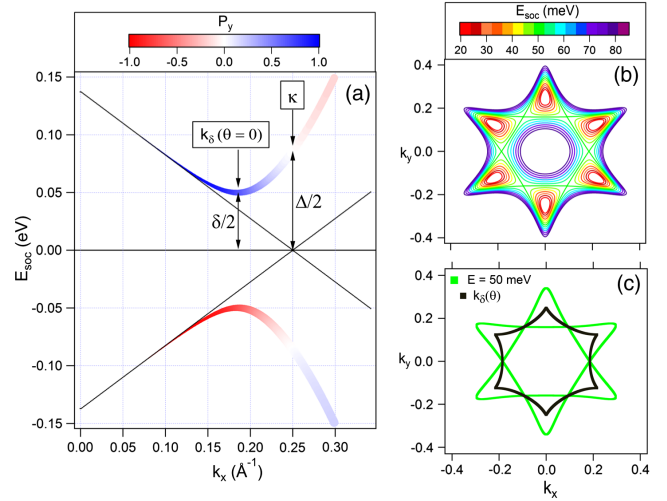


FIG. 2 (color online). Electron structure given by the model Hamiltonian for parameters stated in the text: band structure near the anticrossing point along $\bar{\Gamma}\bar{K}$ ($k_y = 0$) direction (a). The color scale [(a), inset] indicates the spin polarization in \hat{y} direction, while marker size indicates the degree of z spin polarization. Constant energy contours (CECs) of the upper Dirac branch (b). The color scale [(b), inset] indicates the energy E of each contour measured with respect to the Dirac point. The momentum-space contour of the gap minimum overlaid onto the CEC at the Lifshitz transition energy is shown in (c).

the z polarization is 100% and then attenuates to $\sim 90\%$ for $k > \kappa$, where the spin helicity has reversed. The scenario of competing SOC interactions takes place throughout the SBZ, resulting in unusual CEC shapes and topologies, displayed in panel 2(b). If the electron dispersion were determined solely by the SOC in this model, there would exist two Lifshitz points [21] in the chemical potential located at $\mu = \pm E(k_{\delta}, \theta = 0)$. At these points, the Fermi surface topology changes from six pockets enclosing the TSS degeneracies to one electron pocket and one hole pocket enclosing $\bar{\Gamma}$. Near a Lifshitz point, straight edges in the CECs are centered on the $\bar{\Gamma}\bar{M}$ direction, opposite of what would be expected for simple, gapless TSS on a (111) surface [18]. This same pattern appears in CECs probed by ARPES, described in Fig. 3(c) below.

Figure 3 shows the ARPES spectra of the terraced surface of $\text{Bi}_4\text{Se}_3(111)$ collected using 70 eV photons. Previous photoemission electron microscopy studies revealed that surface is terminated by Bi_2 and Bi_2Se_3 layers which are present in approximately equal proportion [10]. The Fermi surface in panel 3(a) has three distinct branches enclosing $\bar{\Gamma}$. It was previously determined that the circular, innermost branch is derived from bulk conduction electrons and Bi_2 surface electrons, while the hexagonal branch outside of that is derived from Bi_2 surface electrons [10]. The outermost branch is derived from surface electrons of the Bi_2Se_3 termination, which display a three-fold enhancement of intensity due to ARPES matrix element effects.

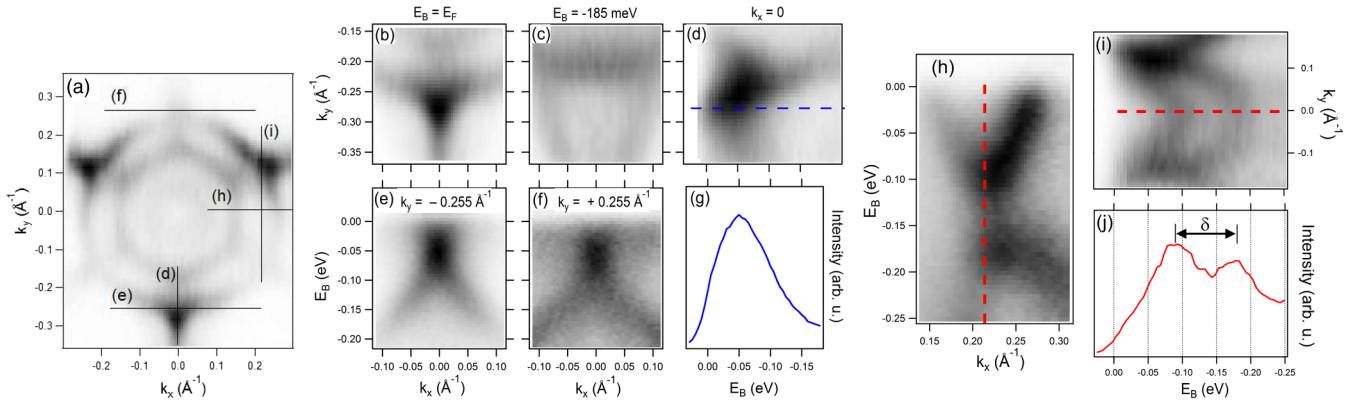


FIG. 3 (color online). ARPES electron structure near the center of the first surface Brillouin zone: the Fermi surface (a),(b), and constant energy contour at -185 meV (c). Band structure parallel to $\bar{\Gamma}\bar{M}$ direction for $k_x = 0$ (d) and $k_x = 0.21 \text{ \AA}^{-1}$ (i). Band structure parallel to $\bar{\Gamma}\bar{K}$ direction at $k_y = -0.255 \text{ \AA}^{-1}$ (e), $k_y = 0.255 \text{ \AA}^{-1}$ (f), and $k_y = 0$ (h). Energy distribution curves at the degeneracy point $(k_x, k_y) = (0, -0.255) \text{ \AA}^{-1}$ (g) and the saddle point of the lower Dirac branch $(k_x, k_y) = (0.21, 0) \text{ \AA}^{-1}$ (j). The momentum-space locations for panels (d),(e) and (h),(i) are indicated by lines overlaid onto the Fermi surface in (a). The gray scale varies from white to black following the minimum-to-maximum photoemission intensity within each image individually.

The degeneration of TSS on the mirror-invariant $\bar{\Gamma}\bar{M}$ ($k_x = 0$) line in the vicinity of $k_y = \pm 0.255 \text{ \AA}^{-1}$ at $E_B = -0.05$ eV is observed in the band structure shown in panels 3(d)–3(f). Crucially, the band structure at $k_y = +0.255 \text{ \AA}^{-1}$ (e) and $k_y = -0.255 \text{ \AA}^{-1}$ (f) appears to be identical, confirming that these bands consist of spin-polarized surface states, which have a six-fold symmetry on the underlying three-fold-symmetric lattice as required by TRS. Comparing the Fermi surface in panel 3(b) to that of the -185 meV CEC [Fig. 3(c)], we observe the formation of a teardrop-shaped CEC that possesses a straight edge centered on $\bar{\Gamma}\bar{M}$, similar to what is predicted by the model Hamiltonian. Panels 3(h)–3(j) reveal a saddle point in the LDB near $(k_x, k_y) = (0.21, 0) \text{ \AA}^{-1}$ (indicated by red dashed lines), where the minimum energy separation δ between the DBs reaches a maximum value (with respect to the in-plane azimuthal angle) of 85 meV. Comparing 3(h)–3(i), it is clear that the LDB reaches a minimum with respect to k_x and a maximum with respect to k_y at this point. This would yield a van Hove singularity [22] in the density of states. Interestingly, the UDB is at a local minimum with respect to both variables at the same point in momentum space. The model Hamiltonian, which retains particle-hole symmetry, predicts a saddle point in both DBs.

The observation of gapped surface states on a (111) surface with large SOC is not without precedent, having been previously identified in heterostructures with BiAg₂ surface alloys [23]; however, the mechanism for the “interband SOC” between the antiparallel, spin-helical surface states in that case was left unspecified. The two-term model Hamiltonian approach shown in this work could be extended to describe not only BiAg₂ surface states, which are known to have a sizable coupling to the in-plane crystal potential gradient [24], but also many other systems, whether topologically trivial or not, in which

spin-helical states intersect away from Kramer’s momenta, such as Pb quantum wells [25]. TIM, rather than topologically trivial materials, may offer more robust platforms for studying this type of spin-gap physics in 2D electron systems. What is lacking at this time is a straightforward and reliable way of predicting if a given STI surface will possess gapped TSS. The present results indicate a need to merge different conceptualizations of the topological insulator (which can be regarded as one and the same with a semimetal in the abstract sense of topological band theory [26]) in order to determine the conditions necessary for this phenomenon.

Some have pointed out [13,14,27] that several well-known TIM possess bulk electron structure that can be characterized as topologically nontrivial using separate methods. The parity-invariant method is used to characterize Z_2 topological insulators [11,12], which include STIs, while mirror topological crystalline insulators (TCIs) are characterized by a nonzero difference in the number of counterpropagating “edge states” corresponding to a crystallographic mirror plane [13,28,29]. Teo, Fu, and Kane [13] had considered that the crossing of TSS at non-TRIM was a possibility for a strong Z_2 topological insulator surface, which motivated them to develop the foundational theory for TCIs. This Letter has presented an experimentally realized case in which the concepts of Z_2 topological insulators and TCIs have become entangled; completely breaking the MS would allow the TSS to become fully gapped, even while TRS remains unbroken. Surely, the significance of the Z_2 topology in determining the electronic physics at *all* of the possible surfaces of a STI should be revisited.

The financial support of the National Science Foundation, Grants No. NSF-DMR-0819860 and No. NSF-DMR-1104612; DARPA-SPAWAR Grant No. N6601-11-1-4110; and the ARO MURI program,

Grant No. W911NF-12-1-0461, are gratefully acknowledged. The Advanced Light Source is supported by the U.S. DOE, Office of Basic Energy Sciences, under Contract No. DE-AC02-05CH11231. Brookhaven National Laboratory is supported by the U.S. Department of Energy, Office of Basic Energy Sciences, Contract No. DE-AC02-98CH10886.

*apwnq5@mail.umkc.edu

- [1] Y. Ando, *J. Phys. Soc. Jpn.* **82**, 102001 (2013).
- [2] M. Z. Hasan and C. L. Kane, *Rev. Mod. Phys.* **82**, 3045 (2010).
- [3] M. Z. Hasan and J. E. Moore, *Annu. Rev. Condens. Matter Phys.* **2**, 55 (2011).
- [4] X. L. Qi and S. C. Zhang, *Rev. Mod. Phys.* **83**, 1057 (2011).
- [5] D. Hsieh, Y. Xia, L. Wray, D. Qian, A. Pal, J. H. Dil, J. Osterwalder, F. Meier, G. Bihlmayer, C. L. Kane, Y. S. Hor, R. J. Cava, and M. Z. Hasan, *Science* **323**, 919 (2009).
- [6] D. Hsieh, L. Wray, D. Qian, Y. Xia, J. H. Dil, F. Meier, L. Patthey, J. Osterwalder, G. Bihlmayer, Y. S. Hor, R. J. Cava, and M. Z. Hasan, *New J. Phys.* **12**, 125001 (2010).
- [7] A. Stróżecka, A. Eiguren, M. Bianchi, D. Guan, C. H. Voetmann, S. Bao, P. Hofmann, and J. I. Pascual, *New J. Phys.* **14**, 103026 (2012).
- [8] M. Bianchi, D. Guan, A. Stróżecka, C. H. Voetmann, S. Bao, J. I. Pascual, A. Eiguren, and P. Hofmann, *Phys. Rev. B* **85**, 155431 (2012).
- [9] T. Valla, H. Ji, L. M. Schoop, A. P. Weber, Z. H. Pan, J. T. Sadowski, E. Vescovo, A. V. Fedorov, A. N. Caruso, Q. D. Gibson, L. Müchler, C. Felser, and R. J. Cava, *Phys. Rev. B* **86**, 241101(R) (2012).
- [10] Q. D. Gibson, L. M. Schoop, A. P. Weber, H. Ji, S. Nadj-Perge, I. K. Drozdov, H. Beidenkopf, J. T. Sadowski, A. Fedorov, A. Yazdani, T. Valla, and R. J. Cava, *Phys. Rev. B* **88**, 081108(R) (2013).
- [11] L. Fu, C. L. Kane, and E. J. Mele, *Phys. Rev. Lett.* **98**, 106803 (2007).
- [12] L. Fu and C. L. Kane, *Phys. Rev. B* **76**, 045302 (2007).
- [13] J. C. Y. Teo, L. Fu, and C. L. Kane, *Phys. Rev. B* **78**, 045426 (2008).
- [14] T. Rauch, M. Flieger, J. Henk, I. Mertig, and A. Ernst, *Phys. Rev. Lett.* **112**, 016802 (2014).
- [15] H. Zhang, C.-X. Liu, X.-L. Qi, X. Dai, Z. Fang, and S.-C. Zhang, *Nat. Phys.* **5**, 438 (2009).
- [16] P. Blaha, K. Schwarz, P. Sorantin, and S. Trickey, *Comput. Phys. Commun.* **59**, 399 (1990).
- [17] J. P. Perdew, K. Burke, and M. Ernzerhof, *Phys. Rev. Lett.* **77**, 3865 (1996).
- [18] L. Fu, *Phys. Rev. Lett.* **103**, 266801 (2009).
- [19] O. V. Yazyev, J. E. Moore, and S. G. Louie, *Phys. Rev. Lett.* **105**, 266806 (2010).
- [20] S. Basak, H. Lin, L. A. Wray, S.-Y. Xu, L. Fu, M. Z. Hasan, and A. Bansil, *Phys. Rev. B* **84**, 121401(R) (2011).
- [21] I. M. Lifshitz, *Sov. Phys. JETP* **11**, 1130 (1960).
- [22] L. van Hove, *Phys. Rev.* **89**, 1189 (1953).
- [23] H. Bentmann, S. Abdelouahed, M. Mulazzi, J. Henk, and F. Reinert, *Phys. Rev. Lett.* **108**, 196801 (2012).
- [24] C. R. Ast, J. Henk, A. Ernst, L. Moreschini, M. C. Falub, D. Pacilé, P. Bruno, K. Kern, and M. Grioni, *Phys. Rev. Lett.* **98**, 186807 (2007).
- [25] B. Slomski, G. Landolt, S. Muff, F. Meier, J. Osterwalder, and J. H. Dil, *New J. Phys.* **15**, 125031 (2013).
- [26] Any material with a band gap that remains open at every point in the Brillouin zone can be regarded as an insulator in the abstractions of topological band theory. The band structure of a semimetal meeting this criterion can be “smoothly deformed” into that of an insulator.
- [27] Y. J. Wang, W.-F. Tsai, H. Lin, S.-Y. Xu, M. Neupane, M. Z. Hasan, and A. Bansil, *Phys. Rev. B* **87**, 235317 (2013).
- [28] L. Fu, *Phys. Rev. Lett.* **106**, 106802 (2011).
- [29] T. H. Hsieh, H. Lin, J. Liu, W. Duan, A. Bansil, and L. Fu, *Nat. Commun.* **3**, 982 (2012).